nature genetics

Transient-mediated fate determination in a transcriptional circuit of HIV

Leor S Weinberger[1,5], Roy D Dar[2,3,5] & Michael L Simpson[2,4]

Steady-state behavior and bistability have been proposed as mechanisms for decision making in gene circuits[1–3]. However, transient gene expression has also been proposed to control cell fate[4,5], with the decision arbitrated by the duration of a transient gene expression pulse. Here, using an HIV-1 model system, we directly quantify transcriptional feedback strength and its effects on both the duration of HIV-1 Tat transcriptional pulses and the fate of HIV-infected cells. By measuring shifts in the autocorrelation of noise inherent to gene expression, we found that transcriptional positive feedback extends the single-cell Tat expression lifetime two- to sixfold for both minimal Tat circuits and full length, actively replicating HIV-1. Notably, artificial weakening of Tat positive feedback shortened the duration of Tat expression transients and biased the probability in favor of latency. Thus, transcriptional positive feedback can modulate transient expression lifetime to a greater extent than protein half-life modulation, and it has a critical role in the cell-fate decision in HIV.

Upon infecting a $CD4^+$ T lymphocyte, the human immunodeficiency virus type 1 (HIV-1) can enter one of two developmental fates: active replication (lysis) or proviral latency (an analog of phage lysogeny). Most infections lead to active replication, destroying the T cell in ~40 h and producing many hundreds of infectious viral progeny[6,7]. A small minority of infections enter proviral latency, a long-lived quiescent state where viral gene expression is turned off[8,9]. Both developmental fates are clinically relevant: active HIV replication destroys the immune system and eventually causes AIDS, and latently infected $CD4^+$ T lymphocytes are the main reservoir thwarting HIV-1 eradication from an affected individual[10]. Although many host factors have been implicated in controlling HIV-1 replication and latency[11–13], the HIV-1 Tat protein (transactivator of transcription) is absolutely essential for active replication and latent reactivation[11,14,15]. Tat transactivation drives active replication by mediating hyperphosphorylation of RNA polymerase II to enhance transcriptional elongation from the long terminal repeat (LTR) promoter of HIV[11,16,17]. Tat transactivation thus comprises an essential positive-feedback loop that drives HIV lytic replication by auto-stimulating its own gene expression 50- to 100-fold above basal levels and simultaneously up-regulating the expression of HIV Rev (the essential viral mRNA export factor) and Nef (a viral protein not essential for viral replication)[18].

We have previously established an HIV-1 model system encoding Tat transcriptional feedback, and we have shown that stochastic fluctuations in Tat gene expression influence a regulatory decision in this circuit[19], and that significant feedback dissipation exists in the Tat feedback loop as a result of the presence of reverse reactions (mediated in part by SirT1) and protein decay[20]. This feedback dissipation architecture stabilizes latency by driving Tat expression pulses that decay to a monostable off-state. However, it was not clear how a circuit that is monostable for one fate (latency) could act as a switch between two cell fates (proviral latency versus active replication). Here, we tested whether positive feedback can modulate the duration of expression transients and thereby mediate a decision between active replication and latency (**Fig. 1**). Specifically, we hypothesized that relatively strong positive feedback generates long-duration Tat transcriptional pulses, which should drive lytic replication and destroy the infected T lymphocyte before the Tat transient decays back to the off-state. Conversely, weaker positive feedback would generate shorter transcriptional pulses, which may bias the probability in favor of latency.

To determine whether positive feedback modulated the Tat expression transient, we used the direct relationship between feedback strength and noise autocorrelation. We carried out noise autocorrelation analysis instead of fluorescence magnitude measurements, as the latter can significantly miscalculate feedback strength, especially when comparisons are being made between different isogenic populations (**Supplementary Methods** online). Using a recently developed gene expression fluctuation autocorrelation theory[21,22], which allows convenient analysis of feedback strength via noise autocorrelation functions (ACF), we measured the strength of Tat positive feedback and estimated the degree of Tat expression pulse extension. Although the noise structure of transcriptional positive feedback has not been previously measured, positive feedback is predicted to increase the correlation time of the noise by an amount related directly to the

[1]Department of Chemistry and Biochemistry, University of California San Diego, 9500 Gilman Drive 0314, La Jolla, California 92093, USA. [2]Center for Nanophase Materials Sciences, Oak Ridge National Laboratory, Bethel Valley Road, Oak Ridge, Tennessee 37831, USA. [3]Departments of Physics and Astronomy and [4]Materials Science and Engineering, University of Tennessee, Knoxville, Tennessee 37996, USA. [5]These authors contributed equally to this work. Correspondence should be addressed to L.S.W. (lsw@ucsd.edu) or M.L.S. (simpsonml1@ornl.gov).

Received 27 August 2007; accepted 26 February 2008; published online 16 March 2008; doi:10.1038/ng.116

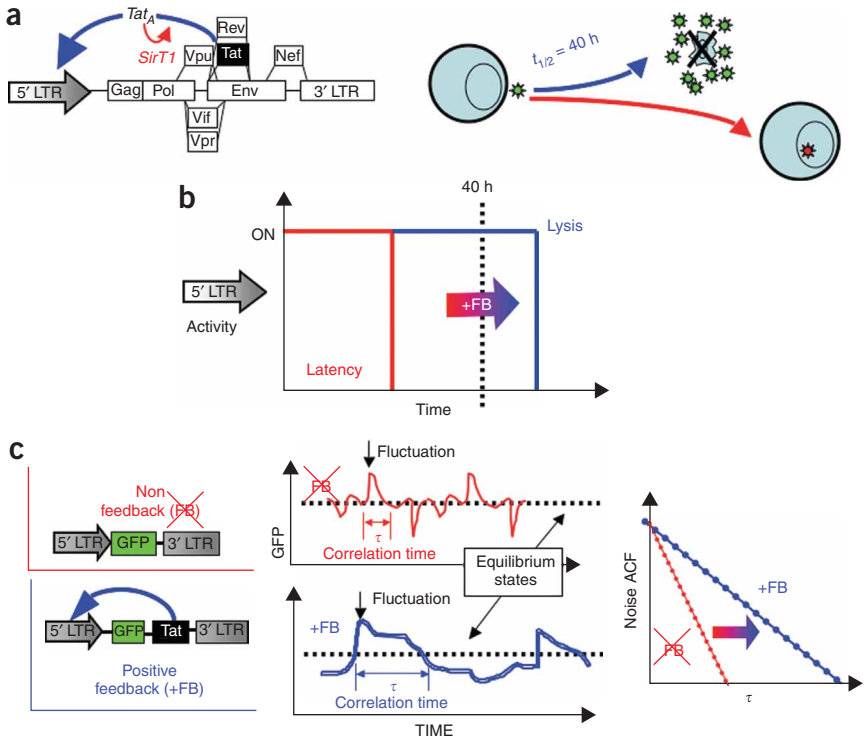

Figure 1 Positive feedback extends the lifetime of gene expression transients. (**a**) The HIV-1 genome encodes the Tat positive-feedback circuit. This circuit is comprised of HIV-1 Tat, which in its short-lived acetylated form (Tat_A) transactivates the viral promoter within the LTR but is also rapidly deacetylated by human SirT1 (refs. 20,30). HIV-infected T cells undergoing active viral replication (that is, with active Tat positive feedback) have an average lifetime of ~40 h[7]. (**b**) Expression transients without positive feedback are short-lived and die out quickly, leading to latency (red). However, positive feedback (in direct proportion to its strength or loop transmission) can extend the duration of gene expression[21] transients, thereby favoring lytic replication (blue). (**c**) Positive-feedback strength can be directly measured in single cells by examining fluctuations in gene expression (left and middle) and calculating a fluctuation autocorrelation function (ACF, right). Positive feedback shifts the ACF decay by a magnitude that correlates directly with the strength of positive feedback[22].

feedback strength. Heuristically, this prediction can be understood by comparing time-series data for minimal HIV circuits with LTR driving GFP (LTR-GFP; no feedback) or GFP and Tat (LTR-GFP-IRES-Tat, hereafter termed LTR-GFP-Tat; positive feedback) expression (**Fig. 1c**, left). Positive feedback reinforces fluctuations away from the mean, which extends the duration of these fluctuations as compared to those from a nonfeedback circuit (**Fig. 1c**, middle). Longer duration fluctuations produce an ACF that decays more slowly (**Fig. 1c**, right), making the ACF width an indicator of positive-feedback strength.

To calculate the noise ACF, we began with observations of GFP fluorescence (observations at times kT_s, $k = 0, 1, 2.....K$) from individually tracked single cells (indexed by m, where $m = 1,2.....$total number of cells tracked; **Supplementary Movie 1** online). We defined noise functions, $\tilde{N}_m(kT_s)$, where the deterministic components (basal and transient) of expression were removed, noise magnitudes were scaled by the total magnitude of expression, and the baselines were suppressed (that is, the $\tilde{N}_m(kT_s)$ functions were zero mean) for the duration of the observation (**Supplementary Methods** and **Supplementary Fig. 1** online). As the durations of observation were by necessity time limited, the $\tilde{N}_m(kT_s)$ functions were missing low-frequency components of the noise. However, we derived normalized high-frequency ACFs ($\Phi_m(jT_s)$), referred to as ACFs in the remainder of the text (**Supplementary Methods**, **Supplementary Fig. 1** and **Supplementary Fig. 2** online), where jT_s varied between 0 and KT_s. We calculated composite ACFs by averaging individual-cell ACFs over the entire population of tracked cells, and we calculated feedback strength, T, from a comparison between $\tau_{1/2}$ values ($\Phi_m(\tau_{1/2}) = 0.5$) for feedback (FB) and nonfeedback (nonFB) cases. The feedback strength (T) was estimated from the relationship $T \rightarrow 1 - (\tau_{1/2\_nonFB}/\tau_{1/2\_FB})$ where the arrow ($\rightarrow$) represents an equality for true ACFs[22] and a mapping operator for high-frequency ACFs (**Supplementary Methods**, **Supplementary Fig. 3** and **Supplementary Table 1** online). Negative values of T indicate negative feedback, and positive values indicate positive feedback that will increase the ACF $\tau_{1/2}$ ($\tau_{1/2\_FB} > \tau_{1/2\_nonFB}$). Similarly, positive feedback also extends the duration of transient excursions by $1/(1-T)$[21,22].

We measured feedback strength in a minimal HIV LTR-GFP-Tat circuit[19] from single-cell gene-expression (that is, GFP intensity) fluctuations (**Fig. 2a**). Noise ACFs for the LTR-GFP-Tat circuit and a nonfeedback LTR-GFP control circuit were compared to minimize the effect of nonbiological (instrumental) noise in both the absence or presence of exogenous Tat protein stimulation (**Fig. 2b**,**c**) and tumor necrosis factor-α (TNF-α; **Supplementary Fig. 4** online) stimulation[23–25]. In all cases, the measured shift in ACF showed that Tat positive feedback increased the duration of transient Tat expression pulses by at least 60% and possibly by as much as tenfold (**Supplementary Methods**). Furthermore, downmodulation of Tat positive feedback by SirT1 overexpression, or using a previously characterized Tat mutant[19,20] (K→A substitution at amino acid 50), led to considerably reduced feedback strength (**Fig. 2d**). Of note, weaker positive feedback correlated with a significantly quicker decay of the LTR expression transient and Tat protein levels (**Fig. 2e** and **Supplementary Fig. 5** online), and although this change in transient duration could be explained by numerous biological mechanisms other than change in positive-feedback strength (for example, active repression of the LTR by an unknown molecular species), ACF analysis indicates that decreased positive-feedback strength is responsible for this effect. Cumulatively, these data experimentally validate the previous theoretical prediction[21,22,26] that positive feedback increases the duration of gene-expression fluctuations, and demonstrate how positive feedback extends the lifetime of transient pulses of gene expression.

Next, we measured how feedback strength correlated with Tat expression duration in both the minimal LTR-GFP-Tat circuit and a previously characterized full-length HIV-1 provirus[11,16] containing GFP cloned in place of Nef (**Fig. 3a**,**b**). As Tat, Rev and Nef (now GFP) are alternatively spliced from one mRNA[27], GFP is a reporter for Tat in this system. We found that full-length HIV-1 showed positive-feedback strength similar to that in the minimal LTR-GFP-Tat circuits (**Fig. 3b**). Time-lapse microscopy and flow cytometry then showed

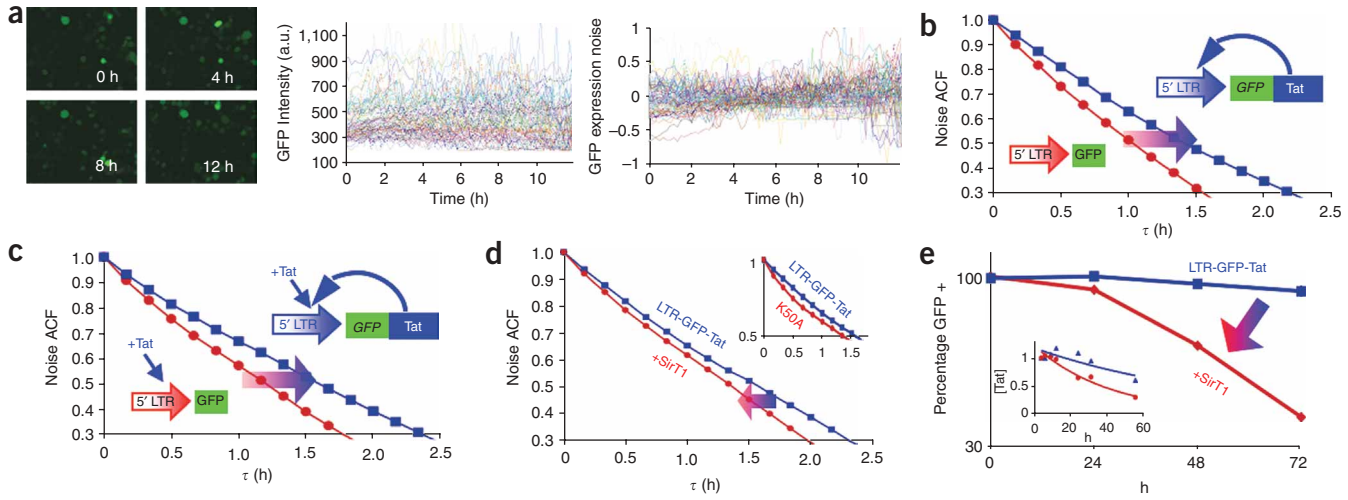

Figure 2 Measuring positive-feedback strength by exploiting inherent gene expression noise. (**a**) Single-cell time-lapse microscopy images of LTR-GFP-Tat isogenic Jurkat T cells over 12 h (left, images captured every 10 mins), single-cell intensity (middle) and processed noise trajectories (right) for determining high-frequency noise autocorrelation functions (ACFs). (**b**) Measured ACFs for LTR-GFP-Tat (ACF $\tau_{1/2} = 1.59 \pm 0.08$ h) and LTR-GFP control (ACF $\tau_{1/2} = 1.2 \pm 0.12$ h); positive feedback shifts HF-ACFs to longer times. (**c**) Measured ACFs after stimulation with exogenous Tat protein for LTR-GFP-Tat (ACF $\tau_{1/2} = 1.77 \pm 0.08$ h) and LTR-GFP control (ACF $\tau_{1/2} = 1.37 \pm 0.10$ h). (**d**) Reducing feedback strength in LTR-GFP-Tat by overexpression of SirT1 (red circle) or via a mutant LTR-GFP-Tat-K50A circuit (inset) decreases ACF shift (ACF $\tau_{1/2} = 1.54 \pm 0.07$ h and 1.55 ± 0.08 h, respectively) compared to wild-type LTR-GFP-Tat circuit (blue diamond; ACF $\tau_{1/2} = 1.76 \pm 0.09$ h). Measurements done after stimulation of positive feedback with TNF-α. (**e**) SirT1 overexpression in LTR-GFP-Tat cells (red) induces two- to sixfold quicker decay in LTR gene expression relative to wild-type LTR-GFP-Tat cells (blue), as measured by flow cytometry for GFP (10^5 cells sorted from the Tat transactivated state at $t = 0$) or quantitative protein blot for Tat protein after 4 h TNF-α stimulation (inset), respectively.

that the expression transient in the minimal LTR-GFP-Tat circuit continued to increase for ~30 h, whereas in full-length HIV-1, the expression transient continued to increase for >40 h (**Fig. 3c**). The half-life of these cells undergoing full-length lytic HIV-1 replication was determined to be $t_{1/2} = 39.5 \pm 5$ h (**Fig. 3d**), which is shorter than the duration of the Tat expression pulse, suggesting that Tat positive feedback strongly biases infected cell fate in favor of lysis.

Next, to test whether the Tat positive-feedback circuit acts as a probabilistic switch with stronger positive feedback increasing the probability of lysis and weaker positive-feedback strength increasing probability of latency, we artificially weakened Tat positive-feedback strength by overexpressing SirT1 in the full-length HIV-1 system. Weakened positive-feedback strength in cells overexpressing SirT1 was confirmed by noise ACF analysis (**Fig. 4a**), and by serial increases in

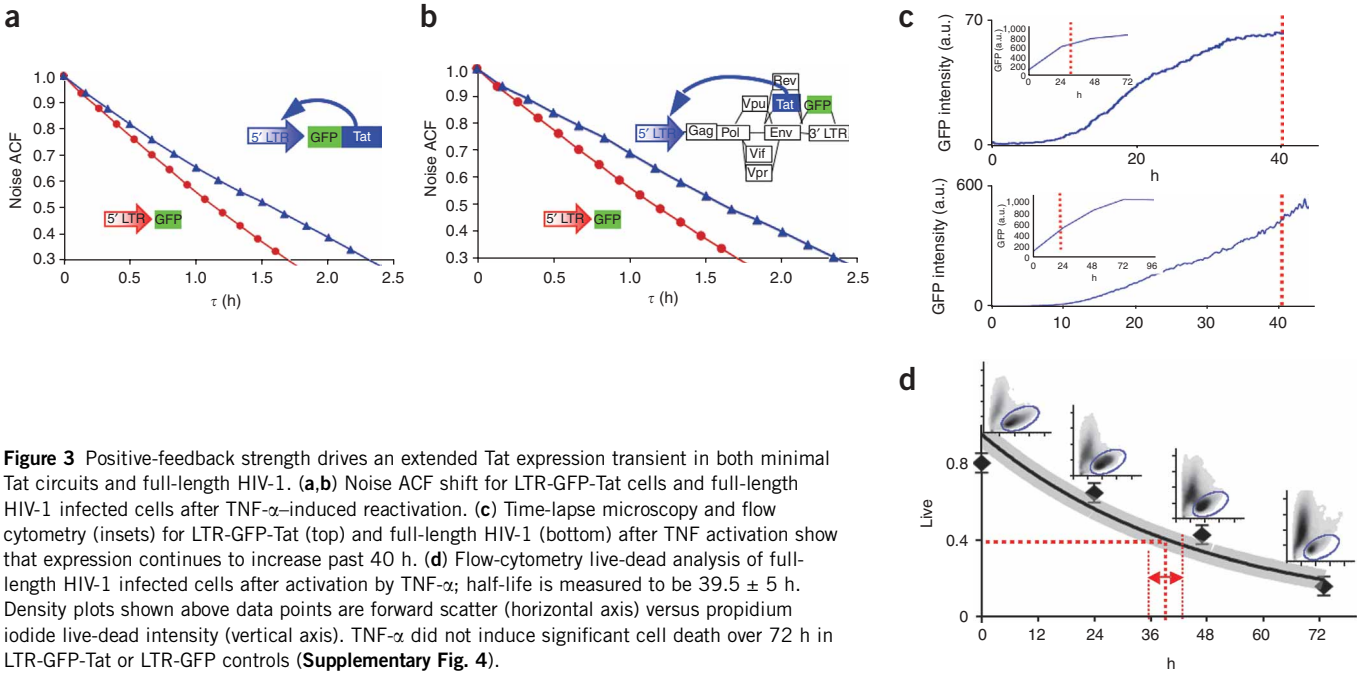

Figure 3 Positive-feedback strength drives an extended Tat expression transient in both minimal Tat circuits and full-length HIV-1. (**a**,**b**) Noise ACF shift for LTR-GFP-Tat cells and full-length HIV-1 infected cells after TNF-α–induced reactivation. (**c**) Time-lapse microscopy and flow cytometry (insets) for LTR-GFP-Tat (top) and full-length HIV-1 (bottom) after TNF activation show that expression continues to increase past 40 h. (**d**) Flow-cytometry live-dead analysis of full-length HIV-1 infected cells after activation by TNF-α; half-life is measured to be 39.5 ± 5 h. Density plots shown above data points are forward scatter (horizontal axis) versus propidium iodide live-dead intensity (vertical axis). TNF-α did not induce significant cell death over 72 h in LTR-GFP-Tat or LTR-GFP controls (**Supplementary Fig. 4**).

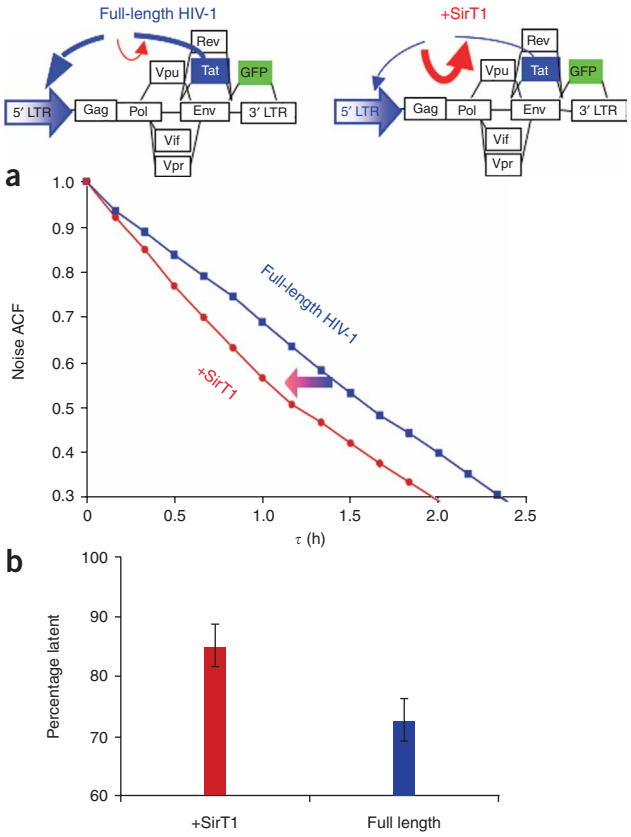

Figure 4 SirT1 overexpression in full-length HIV-1 decreases positive-feedback strength and increases the probability of latency. (**a**) Noise ACF for full-length HIV-1 (blue) and SirT1 overexpression in full-length HIV-1 (red). SirT1 overexpression yields weaker positive-feedback strength compared to full-length HIV-1 alone ($\tau_{1/2} = 1.35 \pm 0.08$ versus $\tau_{1/2} = 1.76 \pm 0.08$, respectively). (**b**) Analytical flow cytometry data showing percentage of latent cells (that is, the percentage of cells not expressing GFP) from triplicate sorts collected 96 h post FACS sorting of TNF-α–activated populations of SirT1 overexpressing (red) and full-length HIV-1 (blue) sorts. SirT1 overexpression results in a significantly higher percentage of latent cells post-transactivation. Error bars are ± 1 s.d., as found from triplicate runs of the same experiment.

SirT1 overexpression that generated successive reductions in activated proviral gene expression (**Supplementary Fig. 6** online). Cells overexpressing SirT1 with weakened Tat positive feedback showed significantly increased probability toward latency (**Fig. 4b**). These data support a model where Tat positive-feedback strength and the resulting transcriptional pulse mediate a probabilistic switch whose outcome may be tuned by cellular modulation of feedback strength (for example, SirT1 activity). Specifically, strong Tat positive feedback extends the lifetime of the transcriptional pulse, leading to HIV-1 lytic replication with very high probability (**Fig. 1b**), whereas weakened positive feedback allows for shorter-lived transcriptional pulses that increase the probability of latency.

At the core, the architecture of this HIV Tat circuit is a transient pulse generator whose duration can be controlled by variable strength, nonlatching, positive feedback over periods that greatly exceed cell division times. Expression transients mediated by long protein half-lives cannot achieve a similar type of modulation, as the dilution effects of cell growth and division ultimately limit transient duration. Where dilution effects are especially significant (for example, in bacterial systems) similar positive-feedback pulse duration mechanisms may be used to tune cell fate determination, such as in the recently reported *Bacillus subtilis* competence decision circuit[5]. Circuit architecture can also affect decision timing: in bistable circuits, such as bacteriaphage λ lysis-lysogeny, the fate decision is made early, whereas the execution occurs much later[28]. Conversely, circuits employing positive feedback–driven transients allow the fate decision to be distributed (that is, integrated) over a much longer period of time, with decision and execution essentially happening simultaneously. Understanding the mechanisms underlying gene circuit and cell-fate decisions may ultimately inform therapy strategies[29]; indeed, modulating Tat positive-feedback strength to bias the lysis-latency decision for therapeutic benefit may represent one such strategy.

METHODS

Constructs and clones. The LTR-GFP and LTR-GFP-Tat constructs are lentiviral vectors whose cloning we have previously described[19]. The LTR-GFP-Tat positive-feedback construct described in this study encodes an internal ribosomal entry sequence (IRES) between GFP and Tat in order to allow bicistronic and stoichoimetrically linked expression of GFP and Tat from a single mRNA. These lentiviral constructs were used to create stable isogenic Jurkat T-cell lines containing single integrations as previously described[19]. The J-lat clonal cell line (J-Lat full-length clone 10.6) was obtained through the US National Institutes of Health AIDS Research and Reference Reagent Program, Division of AIDS, National Institute of Allergy and Infectious Diseases, US National Institutes of Health from E. Verdin[11].

Single-cell time-lapse microscopy and flow cytometry. Jurkat T-cells were imaged on a Perkin-Elmer UltraView spinning disk confocal microscope fitted with a live-cell chamber (Bioptechs). We carried out all experiments at 37 °C under CO_2 using a ×10 dry or heated ×20 immersion objective. We immobilized cells by incubation in glass-bottom cell-culture dishes (Matek) for 1 h, applied drug perturbations and captured images every 5–10 min for 12–15 h at an acquisition speed of 100–1000 msec depending on the experiment. We acquired images and movies using the Perkin-Elmer UltraView software, and we used custom Matlab (Mathworks) code to perform single-cell segmentation and tracking (**Supplementary Movie 1**). We have previously described this technique[20,22].

Flow cytometry and FACS sorting parameters were as follows: living cells (in growth media) were gated on forward versus side scattering and sorted according to the level of GFP expression. We recorded at least 10,000 GFP events for each experiment and analyzed data using FlowJo (Treestar).

Cell culture and drug perturbations. We maintained Jurkat T cells at densities between 2×10^5 to 2×10^6 cells/ml at 37 °C under CO_2 and humidity in RPMI 1640 supplemented with 10% FCS. The LTR-GFP-Tat Jurkat clone E7 and LTR-GFP Jurkat clones D5 and E11 were used throughout this study. These clones have been previously characterized[19]. We dissolved TNF-α (Sigma) in DMSO for a final concentration of 10 ng/ml and obtained purified HIV-1 Tat protein (ABL), and we exposed cells to these perturbations as previously described[14]. We assayed cell death by forward scatter versus side scatter (and propidium-iodide uptake) flow cytometry analysis, and we did not find TNF-α to be significantly cytotoxic to Jurkat cells over 48 h, as is shown for LTR-GFP cells after TNF-α exposure (**Supplementary Fig. 4**).

Quantitative protein analysis. Quantitative protein blot analysis for Tat and GFP was done as previously described[20]. Jurkat cells were activated with TNF-α for 4 h and washed 2× in PBS, and an aliquot of 6×10^6 cells was removed and frozen at the indicated time points. We used the Lowry assay to load equivalent amounts of protein to each well on a 14% gel, and we used an antibody to FLAG to quantify Tat (LTR-GFP-Tat contains a 2× FLAG tag on the 3′ terminus of Tat). After transfer to a membrane, blocking, washing and staining with ECL Plus reagent, blots were quantified on a Molecular Dynamics Typhoon imager.

We normalized band intensities relative to the α-tubulin control (Santa Cruz #5286; antibody to mouse, used at 1:5000) and to the 4 h TNF timepoint (**Supplementary Fig. 5**).

Note: Supplementary information is available on the Nature Genetics website.

ACKNOWLEDGMENTS

We thank D. Botstein, T. Shenk, T. Cox, N. Wingreen, A. Caudy, D. Spector, M. Doktycz, J. Cooke and P. Cummings for helpful comments and S. Werner for technical expertise. The J-lat clonal cell line (J-lat full-length clone 10.6) was obtained through the US National Institutes of Health AIDS Research and Reference Reagent Program, Division of AIDS, National Institute of Allergy and Infectious Diseases, US National Institutes of Health from E. Verdin. L.S.W. acknowledges support from the University of California San Diego and the Lewis Thomas Fellowship (Princeton University). R.D.D. and M.L.S. acknowledge support from the Center for Nanophase Materials Sciences, which is sponsored by the Division of Scientific User Facilities, Office of Basic Energy Sciences, US Department of Energy.

AUTHOR CONTRIBUTIONS

L.S.W., R.D.D. and M.L.S. conceived and designed this study; L.S.W. carried out the single-cell imaging; R.D.D. analyzed the cell images and did the simulations; M.L.S. carried out the analytical derivations; and L.S.W., R.D.D. and M.L.S. wrote the paper.

Published online at http://www.nature.com/naturegenetics
Reprints and permissions information is available online at http://npg.nature.com/reprintsandpermissions

1. Ozbudak, E.M., Thattai, M., Lim, H.N., Shraiman, B.I. & Van Oudenaarden, A. Multistability in the lactose utilization network of *Escherichia coli*. *Nature* **427**, 737–740 (2004).
2. Arkin, A., Ross, J. & McAdams, H.H. Stochastic kinetic analysis of developmental pathway bifurcation in phage lambda-infected *Escherichia coli* cells. *Genetics* **149**, 1633–1648 (1998).
3. Bagowski, C.P. & Ferrell, J.E. Jr. Bistability in the JNK cascade. *Curr. Biol.* **11**, 1176–1182 (2001).
4. Suel, G.M., Garcia-Ojalvo, J., Liberman, L.M. & Elowitz, M.B. An excitable gene regulatory circuit induces transient cellular differentiation. *Nature* **440**, 545–550 (2006).
5. Maamar, H., Raj, A. & Dubnau, D. Noise in gene expression determines cell fate in *Bacillus subtilis*. *Science* **317**, 526–529 (2007).
6. Seth, N., Kaufmann, D., Lahey, T., Rosenberg, E.S. & Wucherpfennig, K.W. Expansion and contraction of HIV-specific CD4 T cells with short bursts of viremia, but physical loss of the majority of these cells with sustained viral replication. *J. Immunol.* **175**, 6948–6958 (2005).
7. Perelson, A.S., Neumann, A.U., Markowitz, M., Leonard, J.M. & Ho, D.D. HIV-1 dynamics in vivo: virion clearance rate, infected cell life-span, and viral generation time. *Science* **271**, 1582–1586 (1996).
8. Finzi, D. *et al.* Identification of a reservoir for HIV-1 in patients on highly active antiretroviral therapy. *Science* **278**, 1295–1300 (1997).
9. Chun, T.W. *et al.* Presence of an inducible HIV-1 latent reservoir during highly active antiretroviral therapy. *Proc. Natl. Acad. Sci. USA* **94**, 13193–13197 (1997).
10. Pierson, T., McArthur, J. & Siliciano, R.F. Reservoirs for HIV-1: mechanisms for viral persistence in the presence of antiviral immune responses and antiretroviral therapy. *Annu. Rev. Immunol.* **18**, 665–708 (2000).
11. Jordan, A., Bisgrove, D. & Verdin, E. HIV reproducibly establishes a latent infection after acute infection of T cells in vitro. *EMBO J.* **22**, 1868–1877 (2003).
12. Lassen, K.G., Ramyar, K.X., Bailey, J.R., Zhou, Y. & Siliciano, R.F. Nuclear retention of multiply spliced HIV-1 RNA in resting CD4 T cells. *PLoS Pathog.* **2**, e68 (2006).
13. Tyagi, M. & Karn, J. CBF-1 promotes transcriptional silencing during the establishment of HIV-1 latency. *EMBO J.* **26**, 4985–4995 (2007).
14. Jordan, A., Defechereux, P. & Verdin, E. The site of HIV-1 integration in the human genome determines basal transcriptional activity and response to Tat transactivation. *EMBO J.* **20**, 1726–1738 (2001).
15. Lin, X. *et al.* Transcriptional profiles of latent human immunodeficiency virus in infected individuals: effects of Tat on the host and reservoir. *J. Virol.* **77**, 8227–8236 (2003).
16. Han, Y., Wind-Rotolo, M., Yang, H.C., Siliciano, J.D. & Siliciano, R.F. Experimental approaches to the study of HIV-1 latency. *Nat. Rev. Microbiol.* **5**, 95–106 (2007).
17. Lassen, K., Han, Y., Zhou, Y., Siliciano, J. & Siliciano, R.F. The multifactorial nature of HIV-1 latency. *Trends Mol. Med.* **10**, 525–531 (2004).
18. Cullen, B.R. Nuclear mRNA export: insights from virology. *Trends Biochem. Sci.* **28**, 419–424 (2003).
19. Weinberger, L.S., Burnett, J.C., Toettcher, J.E., Arkin, A.P. & Schaffer, D.V. Stochastic gene expression in a lentiviral positive-feedback loop: HIV-1 Tat fluctuations drive phenotypic diversity. *Cell* **122**, 169–182 (2005).
20. Weinberger, L.S. & Shenk, T. An HIV feedback resistor: auto-regulatory circuit deactivator and noise buffer. *PLoS Biol.* **5**, e9 (2007).
21. Simpson, M.L., Cox, C.D. & Sayler, G.S. Frequency domain analysis of noise in autoregulated gene circuits. *Proc. Natl. Acad. Sci. USA* **100**, 4551–4556 (2003).
22. Austin, D.W. *et al.* Gene network shaping of inherent noise spectra. *Nature* **439**, 608–611 (2006).
23. Folks, T.M. *et al.* Tumor necrosis factor alpha induces expression of human immunodeficiency virus in a chronically infected T-cell clone. *Proc. Natl. Acad. Sci. USA* **86**, 2365–2368 (1989).
24. Bohnlein, E. *et al.* The same inducible nuclear proteins regulates mitogen activation of both the interleukin-2 receptor-alpha gene and type 1 HIV. *Cell* **53**, 827–836 (1988).
25. Tong-Starkesen, S.E., Luciw, P.A. & Peterlin, B.M. Signaling through T lymphocyte surface proteins, TCR/CD3 and CD28, activates the HIV-1 long terminal repeat. *J. Immunol.* **142**, 702–707 (1989).
26. Cox, C.D. *et al.* Frequency domain analysis of noise in simple gene circuits. *Chaos* **16**, 026102 (2006).
27. Klotman, M.E. *et al.* Kinetics of expression of multiply spliced RNA in early human immunodeficiency virus type 1 infection of lymphocytes and monocytes. *Proc. Natl. Acad. Sci. USA* **88**, 5011–5015 (1991).
28. Alon, U. *An Introduction to Systems Biology: Design Principles of Biological Circuits.* (Chapman & Hall/CRC, Boca Raton, Florida, 2007).
29. Weinberger, L.S., Schaffer, D.V. & Arkin, A.P. Theoretical design of a gene therapy to prevent AIDS but not human immunodeficiency virus type 1 infection. *J. Virol.* **77**, 10028–10036 (2003).
30. Pagans, S. *et al.* SIRT1 regulates HIV transcription via Tat deacetylation. *PLoS Biol.* **3**, e41 (2005).